JBC RESEARCH ARTICLE

A novel C-type lectin activates the complement cascade in the primitive oyster *Crassostrea gigas*

Received for publication, March 30, 2021, and in revised form, October 17, 2021 Published, Papers in Press, October 27, 2021,
https://doi.org/10.1016/j.jbc.2021.101352

Jiejie Sun[1,2,‡], **Liyan Wang**[1,2,‡], **Wenwen Yang**[1,2,‡], **Yinan Li**[1,2], **Yingnan Jin**[1,2], **Lingling Wang**[1,2,3,4,*], and **Linsheng Song**[1,2,3,*]

From the [1]*Liaoning Key Laboratory of Marine Animal Immunology, and* [2]*Liaoning Key Laboratory of Marine Animal Immunology & Disease Control, Dalian Ocean University, Dalian, China;* [3]*Southern Laboratory of Ocean Science and Engineering (Guangdong, Zhuhai), Zhuhai, China;* [4]*Dalian Key Laboratory of Aquatic Animal Diseases Prevention and Control, Dalian Ocean University, Dalian, China*

Edited by Gerald Hart

The ancient origin of the lectin pathway of the complement system can be traced back to protochordates (such as amphioxus and tunicates) by the presence of components such as ficolin, glucose-binding lectin, mannose-binding lectin-associated serine protease (MASP), and C3. Evidence for a more primitive origin is offered in the present study on the Pacific oyster *Crassostrea gigas*. C3 protein in *C. gigas* (*Cg*C3) was found to be cleaved after stimulation with the bacteria *Vibrio splendidus*. In addition, we identified a novel C-type lectin (defined as *Cg*CLec) with a complement control protein (CCP) domain, which recognized various pathogen-associated molecular patterns (PAMPs) and bacteria. This protein was involved in the activation of the complement system by binding *Cg*MASPL-1 to promote cleavage of *Cg*C3. The production of cytokines and antibacterial peptides, as well as the phagocytotic ratio of haemocytes in *Cg*CLec-CCP-, *Cg*MASPL-1-, or *Cg*C3-knockdown oysters, decreased significantly after *V. splendidus* stimulation. Moreover, this activated *Cg*C3 participated in perforation of bacterial envelopes and inhibiting survival of the infecting bacteria. These results collectively suggest that there existed an ancient lectin pathway in molluscs, which was activated by a complement cascade to regulate the production of immune effectors, phagocytosis, and bacterial lysis.

The complement system represents one of the most ancient cornerstones of immunity, which plays essential roles in both innate and adaptive immunity. The mammalian complement system consists of many serum proteins involved in a chain reaction of proteolysis and protein complex assembly that leads to the elimination of pathogens. The complement system can be activated by three distinct pathways, including classical, lectin and alternative pathways, and each of them is composed of immune recognition and a common lytic process to the destruction of invading pathogens (1–4). The lectin pathway is thought to be the most primitive complement pathway. It is activated by the binding between mannose-binding lectin (MBL)/ficolin and carbohydrate patterns from pathogens to assemble different MBL-associated serine proteases (MASPs). Complement proteins C2 and C4 are cleaved by MASPs to form C3 convertase complex (C4aC2b), which converts C3 into a variety of products (5, 6) to mediate various processes, including inflammation, phagocytosis, chemotaxis, and cell lysis (7–9).

The origin and evolution of the complement lectin pathway can be traced back to early deuterostomes, such as lamprey and/or hagfish, amphioxus (lancelets) and ascidian (tunicates) (7). The key components of the lectin pathway, including C3, MBL, and MASP, have been identified in lamprey and/or hagfish (7, 10). In lamprey, the lectin pathway can be activated by MBL and MASP to generate C3 cleavage fragments (7, 11) and a subsequently cytolytic response, which is distinct from the mammalian lytic pathway (10, 12–14). A ficolin-mediated complement pathway has been identified in amphioxus, in which MASP1/3 can form complexes with ficolin (FCN1) to facilitate the activation of C3 (11). The more ancient origin of lectin pathway is further proved by the identification of glucose-binding lectin (GBL) (15), MASP, (16) and C3 (17) from ascidian. The GBL from ascidian lacks a collagen-like domain presenting in mammalian MBLs, but it can associate with MASPs to activate C3 and mediate haemocyte phagocytosis (18). These pieces of evidence indicate that the lectin-dependent complement system has been developed in Urochordates and Chordates (19).

The identification of MASP or MASP-like molecule in protostomes suggests that the lectin pathway antedates the classical and alternative pathways of the complement activation. Actually, the existence of complement systems in insects has been controversial for a long time, even the thioester-containing proteins (TEPs) are proved to execute similar functions as mammalian C3 (20). In shrimp *Litopenaeus vannamei*, only one C3-like gene has been identified (21). Although C3 and MASP have been identified in the sea anemone *Nematostella vectensis*, their functions are still not fully defined (22–24). In molluscs, the homologues of C3 have been recently documented in oyster (25), clam (26–28), and

‡ These authors contributed equally to this work.
* For correspondence: Lingling Wang, wanglingling@dlou.edu.cn; Linsheng Song, lshsong@dlou.edu.cn.

mussel (29), which contain all the conservative motifs identified in mammalian C3. Moreover, MASP-like molecule 1 (MASPL-1) lacking complement control protein (CCP) domains was also identified in oyster (30), suggesting that a complement lectin pathway might exist in molluscs. Though MASP has been identified in protostomes, there are still no reports about protostome MBL/ficolin homologues with collagen-like regions. It is suspected that the ancient complement pathway is likely to undergo major changes during evolution (7, 15, 31). At the same time, due to the lack of some key molecules, especially most of the proteins involved in the formation of membrane attack complex (MAC), such as C5, C6, C7, C8, and C9 (32) in early deuterostomes and protostomes, the lectin pathway is suspected to be assembled in some special ways to induce the cytolytic systems, which is different from mammalian ones (7).

Molluscs are protostome animals with evolutionary significance, and they also represent a significant proportion of world aquaculture production, in which the Pacific oyster *Crassostrea gigas* is considered as one of the most important commercial marine species. Recently, a large number of gene models containing complement-related domains have been characterized in oyster *C. gigas*, and C3 has been identified in the cell-free haemolymph as a processed mature protein, suggesting that the complement system might be of significance for the innate immune response of molluscs (25). However, the activation mechanism of the complement system and its functions in molluscs are still not clear. Although hundreds of C-type lectins (CTLs), fibrinogen-related proteins (FREPs), and MASP-like proteins have been found in *C. gigas* (25, 33), there are no homologues sharing similar domain organization with mammalian MBL/ficolin/MASP. These findings encourage us to suspect that the lectin pathway in primitive invertebrates may assemble in flexible ways different from that in vertebrates, in which other paralogous molecules with complement-related domains may be dedicated to the activation cascade. In the present study, a novel C-type lectin was identified from *C. gigas* (designated *Cg*CLec-CCP) with the objectives to confirm the existence of the ancient complement lectin pathway and understand its activation mechanism and roles in antibacterial immunity in molluscs.

Results

The distribution, expression, activation, and antibacterial activity of CgC3 after V. splendidus stimulation

A C3 homologue was found by bioinformatic means from oyster (*Cg*C3) with an A2M_N_2 (Alpha-2-macroglobulin) domain, an A2M (Alpha-2-macroglobulin family) domain, a TBR (Alpha-macro-globulin thiol-ester bond-forming region) domain, an A2Mc (Complement component region of A2M), an A2MR (A-macroglobulin receptor) domain, and an NTR (Netrin) module (Figs. 1*A* and S1). The mRNA transcripts of *Cg*C3 were examined by qRT-PCR, and they were found to be expressed in all the tested tissues with relatively higher expression level in haemocytes, mantle, and adductor muscle (Fig. 1*B*). Haemocytes are the main invertebrate immune cells circulating in a semi open circulatory system containing haemolymph (the circulatory fluid). The relatively expression level of *Cg*C3 mRNA in haemocytes increased significantly at 6, 12, 24, and 48 h after *Vibrio splendidus* stimulation, which were 3.5-fold, 16.6-fold, 8.2-fold, and 6.9-fold than that at 0 h, respectively (Fig. 1*C*). The polyclonal antibody against *Cg*C3-NTR (anti-*Cg*C3) was prepared from mouse, and its specificity was examined by western blotting. There was a distinct band of recombinant His-*Cg*C3-NTR, which was consistent with the predicted molecular weight of His-*Cg*C3-NTR (Fig. 1*D*). A band of *Cg*C3 from cell-free haemolymph of untreated oysters was shown, which was identical to the prediction of molecular mass of *Cg*C3 (Fig. 1*E*). Usually, C3 molecule consists of an α- and a β-chain, which can be cleaved into different fragments. Coimmunoprecipitation with anti-*Cg*C3 revealed that there were four bands (the full-length *Cg*C3, alpha chain of *Cg*C3, alpha chain fragment of i*Cg*C3b, and C3γ fragment) for the proteins from cell-free haemolymph and haemocytes from the oysters stimulated by *V. splendidus* for 30 min (Figs. 1*E* and S1). The mass spectrometric analysis was conducted using the cell-free haemolymph of oysters. Anti-*Cg*C3 antibody was used to immunoprecipitate *Cg*C3 fragments in the cell-free haemolymph from *V. splendidus*-infected oysters, and the proteins were analyzed by SDS-PAGE. The immunoprecipitated *Cg*C3 fragment (alpha chain fragment of iC3b) was identified by mass spectrometric analysis (Beijing Protein Innovation, BPI) (Fig. S2, *A* and *B*). In the immunocytochemistry assay with anti-*Cg*C3, *Cg*C3 was marked with Alexa Fluor 488-labeled Goat Anti-Mouse IgG in green, and nucleus was stained by 4′,6-diamidino-2-phenylindole (DAPI) in blue. The positive signals of *Cg*C3 were mainly distributed in haemocyte cytoplasm, which were transferred to the membrane after *V. splendidus* stimulation, compared with those in phosphate buffered saline (PBS) group (Fig. 1*F*). After *V. splendidus* were incubated with the native complex proteins from oysters coimmunoprecipitated by anti-*Cg*C3 after *V. splendidus* stimulation, the bacteria growth was inhibited, and the OD value decreased significantly from 2 to 5 h, which was 0.7- to 0.8-fold of that in PBS group (Fig. 1*G*). Meanwhile, the envelope of *V. splendidus* was observed to be perforated (Fig. 1*H*).

The molecular features, mRNA expression patterns, and ligand-binding activities of CgCLec-CCP

A C-type lectin (defined as *Cg*CLec-CCP) with a CCP domain and a carbohydrate recognition domain (CRD) domain was identified in oyster *C. gigas* (Fig. 2*A*). A short stretch of the N-terminal nonlectin region in *Cg*CLec-CCP shared limited similarity with the collagen region in MBLs from other species, and six residues (CPD and WPD) in CRD domain of *Cg*CLec-CCP were predicted to be involved in carbohydrate binding (Fig. S3). The mRNA transcripts of *Cg*CLec-CCP were distributed in all tested tissues, with relatively higher abundance in haemocytes and gonad

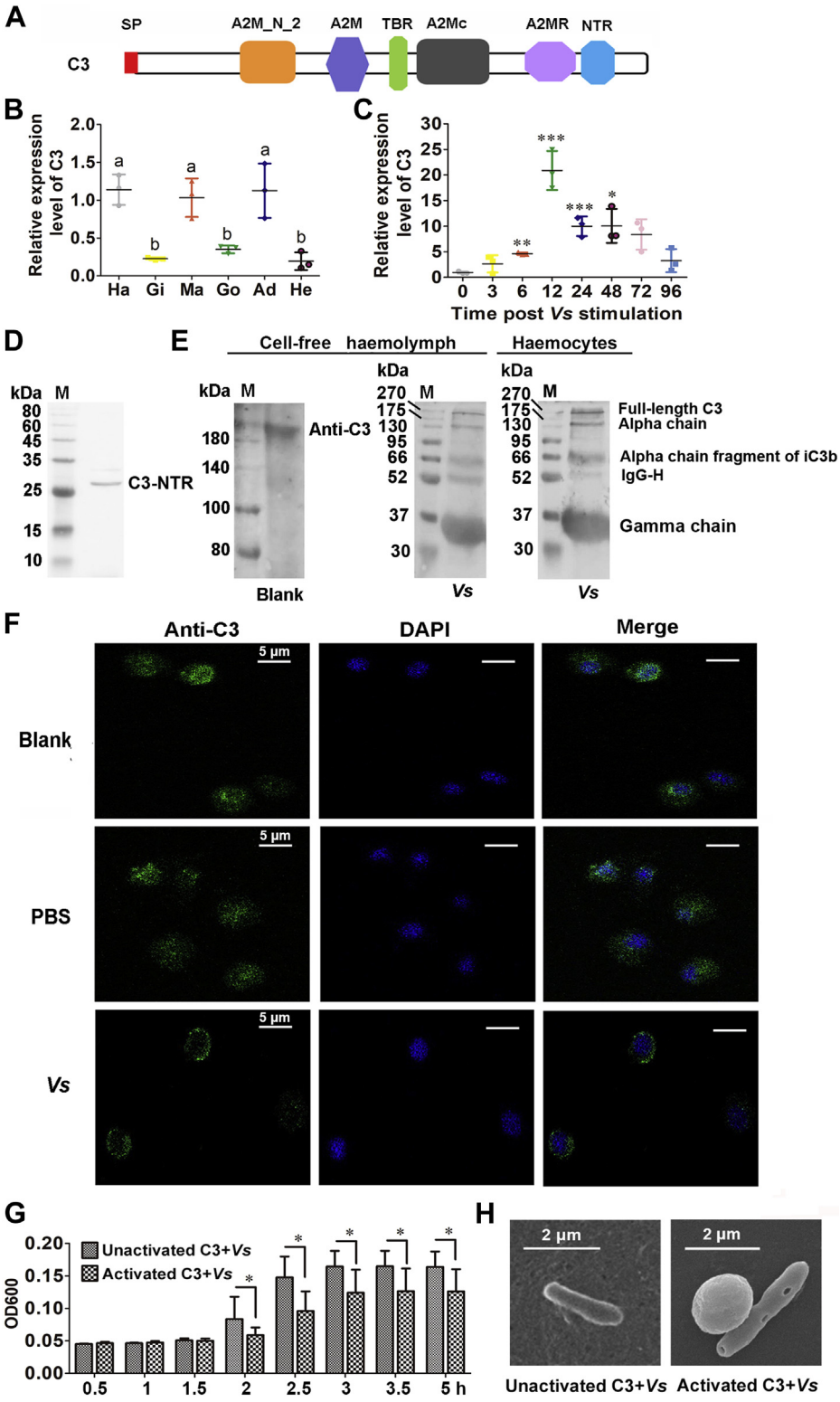

Figure 1. The activation of *Cg*C3 after *V. splendidus* stimulation. *A*, the domain architecture of oyster *Cg*C3. *B*, the distribution of *Cg*C3 mRNA in tissues. Ha, haemolymph; Gi, gills; Ma, mantle; Go, gonad; Ad, adductor muscle; He, hepatopancreas. *C*, the temporal and spatial mRNA expression patterns of *Cg*C3 in haemocytes. *D*, the purification of r*Cg*C3-NTR protein. *E*, detection of *Cg*C3 cleavage in cell-free haemolymph and haemocytes by using anti-*Cg*C3 antibody. *F*, the subcellular location of *Cg*C3 after *V. splendidus* stimulation. *G*, the direct bacteriostatic/bacteriocidal activity of the native complex proteins coimmunoprecipitated by *Cg*C3 antibody after *V. splendidus* stimulation. *H*, SEM image of bacterial cells after incubation with the native complex proteins coimmunoprecipitated by *Cg*C3 antibody after *V. splendidus* stimulation. The sphere next to the bacterium was Protein G Agarose Bead. Data shown were the mean ± SD (n = 3). $*p < 0.05$, $**p < 0.01$ (Student's *t* test). Different letters: $p < 0.05$ (one-way ANOVA).

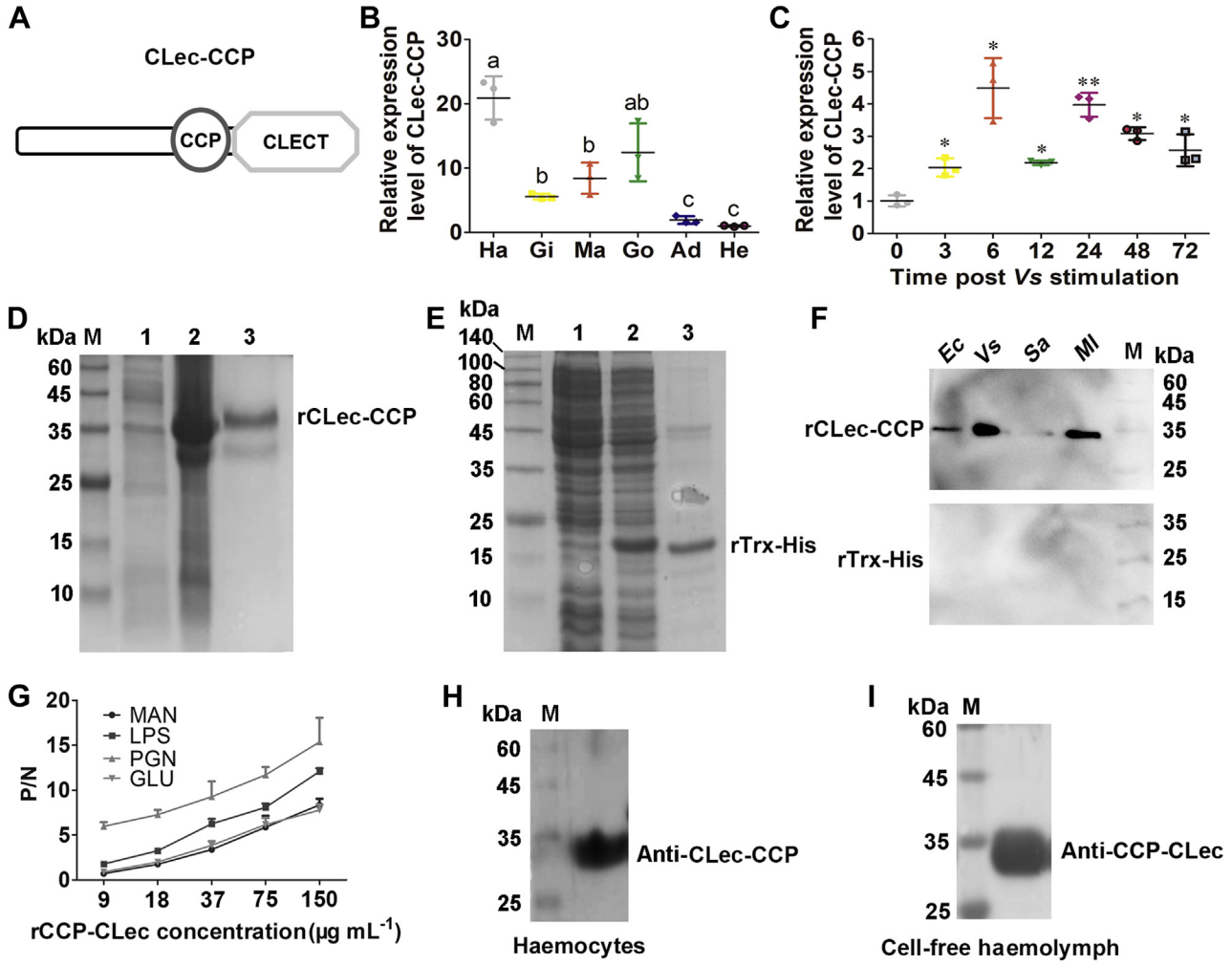

Figure 2. The recognization of *Cg*CLec-CCP to multiple PAMPs and bacteria. *A*, the domain architecture of oyster *Cg*CLec-CCP. *B*, the distribution of *Cg*CLec-CCP mRNA in tissues. *C*, the temporal and spatial mRNA expression patterns of *Cg*CLec-CCP in haemocytes. *D* and *E*, the recombinant expression and purification of rHis-*Cg*CLec-CCP and rTrx-His proteins. Lane M, protein marker; lane 1, the whole cell lysates of positive transformants before induction with IPTG; lane 2, the expressed rHis-*Cg*CLec-CCP and rTrx-His proteins; lane 3, purified rHis-*Cg*CLec-CCP and rTrx-His proteins. *F*, The bacteria-binding activities of rHis-*Cg*CLec-CCP. *G*, PAMP-binding activities of rHis-*Cg*CLec-CCP to LPS, PGN, MAN, and GLU. *H* and *I*, the specific Ab detection of *Cg*CLec-CCP in haemocytes and haemolymph. Data shown were the mean ± SD (n = 3). *$p < 0.05$, **$p < 0.01$ (Student's *t* test). Different letters: $p < 0.05$ (one-way ANOVA).

(21.4-fold and 11.7-fold of that in hepatopancreas, $p < 0.05$, respectively) (Fig. 2*B*). The mRNA expression level of *Cg*CLec-CCP in haemocytes increased significantly at 3, 6, 12, 24, 48, and 72 h after *V. splendidus* stimulation (Fig. 2*C*). The recombinant forms of *Cg*CLec-CCP (rHis-*Cg*CLec-CCP) and Trx-His (rTrx-His) were expressed in *Escherichia coli* and purified by affinity chromatography (Fig. 2, *D* and *E*). r*Cg*CLec-CCP exhibited binding activity toward G^- bacteria (*E. coli* and *V. splendidus*) and G^+ bacteria (*Staphylococcus aureus* and *Micrococcus luteus*) with the relatively higher binding activity to *V. splendidus* and *M. luteus* (Fig. 2*F*). It bound LPS, PGN, MAN, and GLU in a dose-dependent manner and displayed relatively higher binding affinity toward LPS and PGN (Fig. 2*G*). Western blot assay with anti-*Cg*CLec-CCP antibody revealed that there was a distinct band of *Cg*CLec-CCP in both haemocyte and cell-free haemolymph samples (Fig. 2, *H* and *I*).

*Cg*C3 cleavage, haemocyte phagocytosis, and cytokine production after *Cg*CLec-CCP was blocked by the corresponding antibody or knocked down by RNAi

As no definite MBL ortholog had been identified in oysters, the *Cg*CLec-CCP with additional CCP domain was suspected to display the same function as the mammalian MBL. The cleavage of *Cg*C3 was examined after *Cg*CLec-CCP was blocked by its antibody. In the pre-serum-blocked oysters, there were two bands (the full-length *Cg*C3 and alpha chain fragment of i*Cg*C3b) in cell-free haemolymph after *V. splendidus* stimulation, while the band of the full-length *Cg*C3 became thicker and the band of alpha chain fragment of i*Cg*C3b became thinner in anti-*Cg*CLec-CCP antibody-blocked oysters after *V. splendidus* stimulation (Fig. 3*A*). After *Cg*CLec-CCP was knocked down by RNA interference (RNAi) (Fig. 3*B*), the phagocytotic rate toward *V. splendidus* and mRNA transcripts of *Cg*IL17-1 and *Cg*TNF-1 all decreased compared with

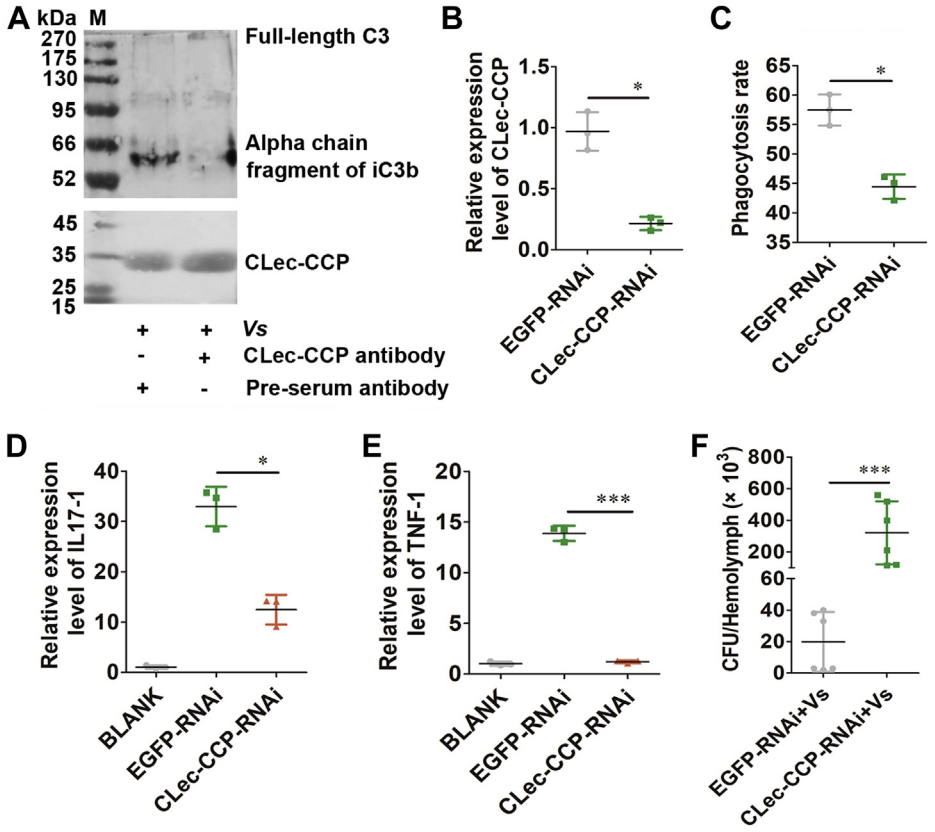

Figure 3. The cleavage of *Cg*C3, haemocyte phagocytosis and immune effector expressions after *Cg*CLec-CCP was blocked or knocked down. *A*, the cleavage of *Cg*C3 in anti-*Cg*CLec-CCP antibody-blocked oysters. *B*, RNAi efficiency of *Cg*CLec-CCP in *Cg*CLec-CCP dsRNA-injection oysters using qRT-PCR. *C*, the phagocytic rate determined by flow cytometry in *Cg*CLec-CCP-RNAi oysters. *D* and *E*, the mRNA transcripts of *Cg*IL17-1 and *Cg*TNF-1 in *Cg*CLec-CCP-RNAi oysters. *F*, the numbers of *V. splendidus* calculated in *Cg*CLec-CCP-RNAi oysters. Dot plots shown were the mean ± SD (n = 3). *$p < 0.05$, **$p < 0.01$, ***$p < 0.001$ (Student's *t* test).

those in EGFP-RNAi oysters, which was 0.8-fold, 0.4-fold, and 0.1-fold ($p < 0.05$) of that in EGFP-RNAi oysters, respectively (Fig. 3, *C–E*). However, the number of *V. splendidus* in the haemolymph increased significantly (16.2-fold of that in EGFP-RNAi oysters, $p < 0.01$) in *Cg*CLec-CCP-RNAi oysters (Fig. 3*F*).

Cg*MASPL-1 and its interaction with* Cg*CLec-CCP and* Cg*C3*

MASP is a member of the lectin pathway of complement, which can be activated by MBL/ficolin to induce the cleavage of C3 in mammals. A MASP-like protein (*Cg*MASPL-1) was identified in oyster with four CUB domains, three LDLs domains, and a Tryp_SPc domain (Figs. 4*A* and S4*A*). Multiple alignment and phylogeny analysis revealed relatively lower conservative property between *Cg*MASPL-1 and MASPs from different species (Fig. S4, *B* and *C*). There were two additional cysteines (Cys683 and Cys808) in *Cg*MASPL-1 to form the "histidine loop" disulfide bridge in its protease domain with the same manner as that in *Hs*MASP1 and *Ms*MASP1 (Fig. S4, *A* and *C*). The mRNA transcripts of *Cg*MASPL-1 were expressed in all tested tissues, with higher level in hepatopancreas (Fig. 4*B*). The expression level of *Cg*MASPL-1 mRNA in haemocytes increased significantly at 6, 12, and 24 h after *V. splendidus* stimulation, which were 10.2-fold, 4.4-fold, and 6.0-fold ($p < 0.05$) of that in Blank group, respectively (Fig. 4*C*). The purified recombinant protein of *Cg*MASPL-1-CUB1 (Fig. 4*D*) was used for pull-down assay. There was a band corresponding to rHis-*Cg*CLec-CCP, while no band was observed in rTrx-His control group (Fig. 4, *E* and *F*). *Cg*MASPL-1 was coimmunoprecipitated by anti-*Cg*CLec-CCP antibodies, and the band of *Cg*MASPL-1 became thicker after *V. splendidus* stimulation, compared with that in PBS group (Fig. 4*G*). The purified rGST-*Cg*MASPL-1-CUB1 was used to bind the native *Cg*C3 from haemolymph. Pull-down assay with anti-*Cg*C3 antibody revealed that there was a band of alpha chain fragment of *Cg*iC3b (Fig. 4*H*). When the haemolymph sample from the oyster stimulated by *V. splendidus* was coimmunoprecipitated with the *Cg*MASPL-1 antibodies, there were four bands observed, which were correspondent to the complex of the full-length *Cg*C3 and *Cg*MASPL-1, the full-length *Cg*C3, alpha chain of *Cg*C3, and alpha chain fragment of i*Cg*C3b, respectively (Fig. 4*I*).

The phagocytotic rate of haemocytes, productions of Cg*IL17-1,* Cg*IL17-2,* Cg*TNF-1, and* Cg*BigDef1 in haemocytes, and number of* V. splendidus *in haemolymph after* Cg*MASPL-1 was knocked down*

RNAi was used to specifically inhibit the expression of *Cg*MASPL-1 in haemocytes at 24 h after the injection of *Cg*MASPL-1 double-stranded RNA (dsRNA). The mRNA

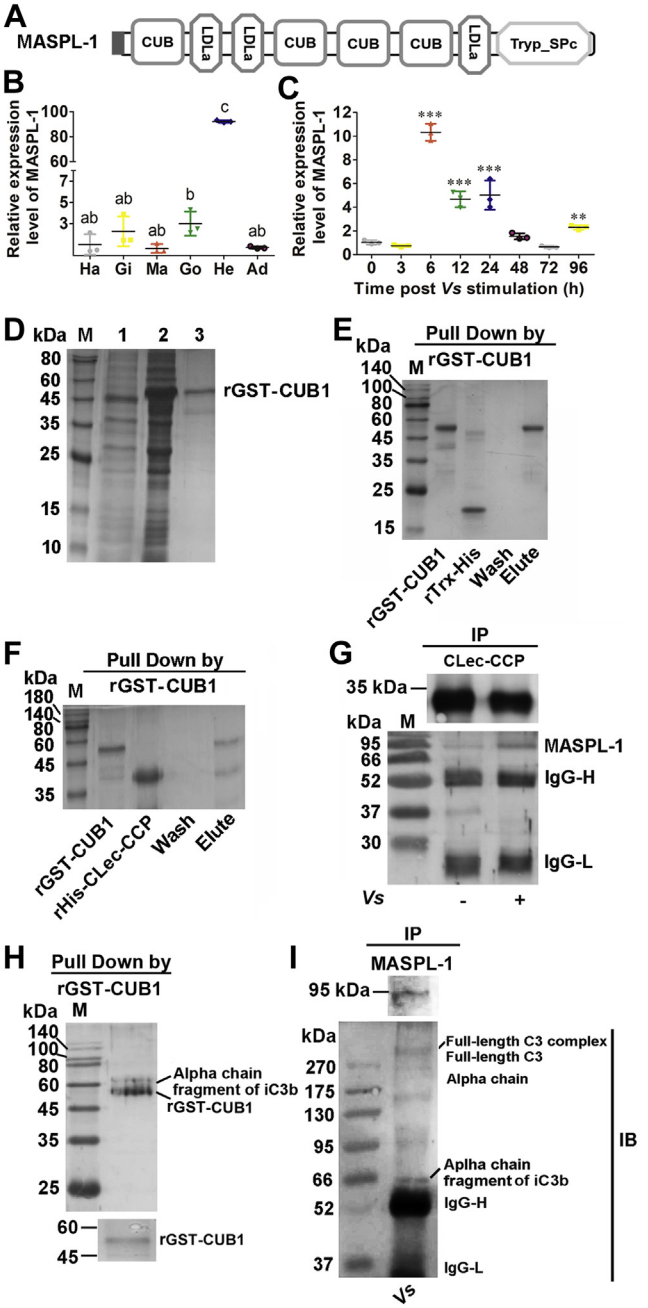

Figure 4. The interaction between *Cg*MASPL-1 and *Cg*CLec-CCP or *Cg*C3 after *V. splendidus* stimulation. *A*, the domain architecture of oyster *Cg*MASPL-1. *B*, the distribution of *Cg*MASPL-1 mRNA in tissues. *C*, the temporal and spatial mRNA expression patterns of *Cg*MASPL-1 in haemocytes. *D*, the recombinant expression and purification of *Cg*MASPL-1-CUB1 (GST-CUB1). Lane M, protein marker; lane 1, the whole cell lysates of positive transformants before induction with IPTG; lane 2, the expressed rGST-CUB1 proteins; lane 3, purified rGST-CUB1 proteins. *E*, the interaction between rGST-CUB1 and rTrx-His. *F*, the interaction between rGST-CUB1 and rHis-*Cg*CLec-CCP. *G*, the interaction between *Cg*MASPL-1 and *Cg*CLec-CCP after *V. splendidus* stimulation. *H*, the interaction between rGST-CUB1 and the alpha chain fragment of *Cg*iC3b. *I*, the interaction between *Cg*MASPL-1 and *Cg*C3 after *V. splendidus* stimulation. Data were the mean ± SD (n = 3). *$p < 0.05$, **$p < 0.01$ (Student's *t* test). Different letters: $p < 0.05$ (one-way ANOVA).

expression level of *Cg*MASPL-1 decreased significantly, which was 0.2-fold lower than that in EGFP-RNAi oysters (Fig. 5*A*). In *Cg*MASPL-1-RNAi oysters, the phagocytotic rate of haemocytes toward *V. splendidus* was 0.5-fold ($p < 0.01$) of that in EGFP-RNAi oysters (Fig. 5, *B* and *C*). Meanwhile, the mRNA expression levels of *Cg*IL17-1, *Cg*IL17-2, *Cg*TNF-1, and *Cg*BigDef1 also decreased significantly, which were 0.1-fold, 0.4-fold, 0.3-fold, and 0.1-fold ($p < 0.05$) of that in EGFP-RNAi oysters, respectively (Fig. 5, *D*–*G*). However, the number of *V. splendidus* in the haemolymph increased significantly, which was 18.4-fold of that in EGFP-RNAi oysters ($p < 0.01$) (Fig. 5*H*).

The phagocytotic rate of haemocytes, productions of Cg*IL17-1,* Cg*IL17-2,* Cg*TNF-1, and* Cg*BigDef1 in haemocytes, and number of* V. splendidus *in haemolymph after* Cg*C3 was knocked down*

The complement lectin pathway is able to induce proinflammatory factor secretion and cytolysis. The phagocytosis and production of some cytokines were determined after *Cg*C3 was knocked down by RNAi. The immunocytochemistry assay by using the anti-*Cg*C3 antibody and FITC-*V. splendidus* was conducted to detect the location of activated *Cg*C3 on the cell surface of *V. splendidus*. *Cg*C3 was labeled with Alexa Fluor 488-labeled Goat Anti-Mouse IgG in red, and nucleus was stained by DAPI in blue. The positive red signals of *Cg*C3 distributed on the cell surface of *V. splendidus*, while no positive signals were observed in the negative control with Preserum (Fig. 6*A*). The expression level of *Cg*C3 mRNA decreased significantly at 24 h after the injection of *Cg*C3 dsRNA, which was 0.48-fold lower than that in EGFP-RNAi oysters (Fig. 6*B*). The number of phagocytized *V. splendidus* in haemocytes was counted by flow cytometry analysis (Fig. 6*C*) to calculate the phagocytotic rate. The phagocytotic rate decreased significantly in *Cg*C3-RNAi oysters (Fig. 6*D*), which was 0.6-fold of that in EGFP-RNAi oysters (Fig. 6, *E* and *F*). Meanwhile, the mRNA expression levels of *Cg*IL17-1, *Cg*IL17-2, and *Cg*BigDef1 all decreased significantly in *Cg*C3-RNAi oysters, which were 0.2-fold, 0.2-fold, and 0.1-fold ($p < 0.05$) of that in EGFP-RNAi oysters, respectively (Fig. 6, *G*–*J*). However, the number of *V. splendidus* in the haemolymph increased significantly (4.1-fold of that in EGFP-RNAi oysters, $p < 0.01$) (Fig. 6*K*).

Discussion

The lectin pathway is one of the well-studied complement activation pathways in vertebrates, which plays significant roles in opsonization of pathogens, chemotaxis, activation of leukocytes, directly killing of pathogens, and modulation of inflammatory (34, 35). It can be triggered by the specific activation cascade, in which MBLs and ficolins firstly recognize PAMPs and subsequently associate with MASPs. The activation of the lectin pathway promotes the cleavage of C3, and the resulting products can bind the invading bacteria and destruct them by lytic pathway (36). The increasing evidence demonstrates that the complement system also exists in invertebrates (31). A number of genes encoding the components in the lectin pathway have been annotated in the genome of ascidian *Ciona intestinalis* and amphioxus *B. floridae* (37, 38), which

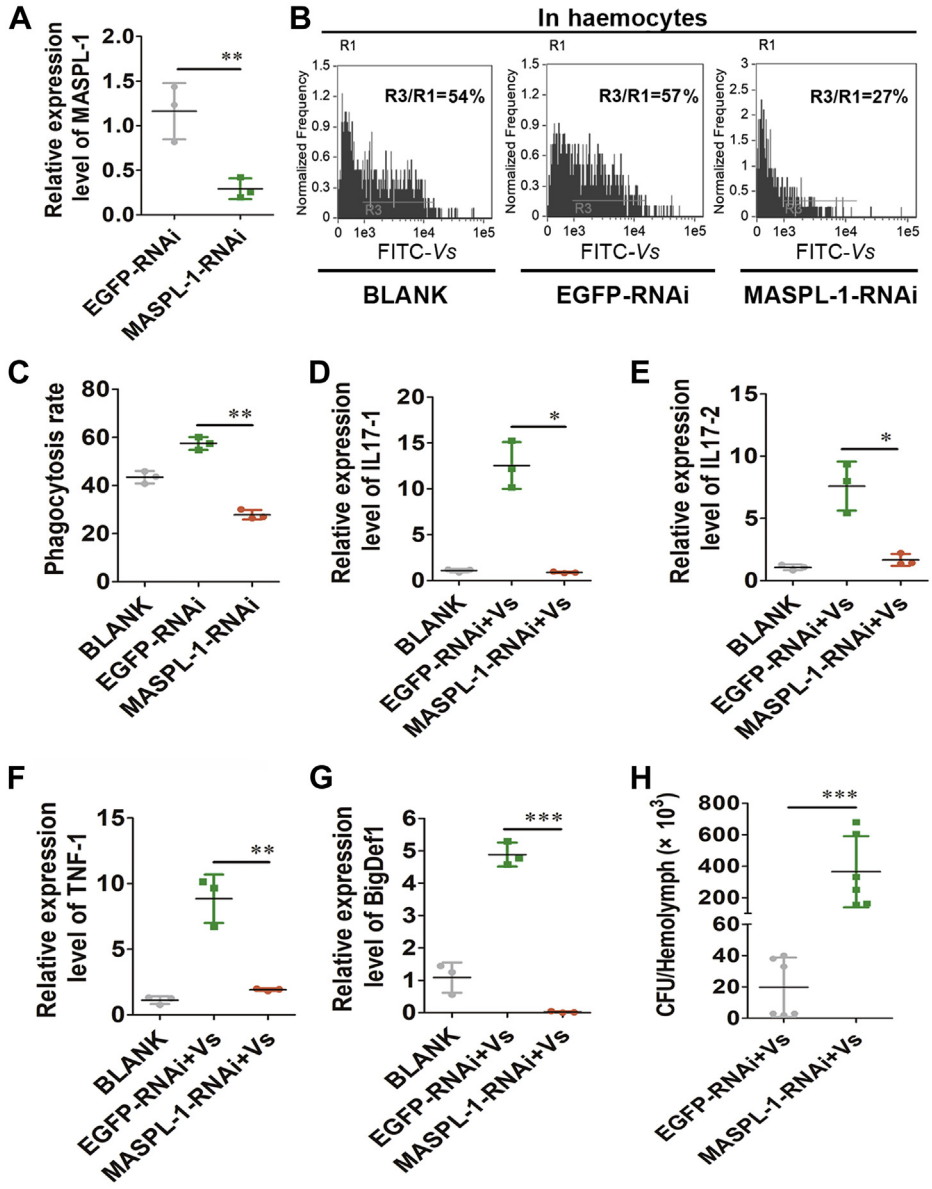

Figure 5. The haemocyte phagocytosis and immune effector expressions after *Cg*MASPL-1 was knocked down. *A*, RNAi efficiency of *Cg*MASPL-1 in *Cg*MASPL-1 dsRNA-injection oysters using qRT-PCR. *B* and *C*, the phagocytic rate determined by flow cytometry in *Cg*MASPL-1-RNAi oysters. *D–G*, the mRNA transcripts of *Cg*IL17-1, *Cg*IL17-2, *Cg*TNF-1, and *Cg*BigDef1 in *Cg*MASPL-1-RNAi oysters after *V. splendidus* stimulation. *H*, the numbers of *V. splendidus* calculated in *Cg*MASPL-1-RNAi oysters. Dot plots shown were the mean ± SD (n = 3). $^{*}p < 0.05$, $^{**}p < 0.01$ (Student's *t* test).

undoubtedly indicates that the lectin pathway can be evolutionary traced back to Urochordata (7, 39). Recently, C3 was characterized to play crucial roles in antibacterial immunity of molluscs (25). However, as the homologues of MASP or MBL/ficolin have not been identified in molluscs, the existence of molluscan lectin pathway is more controversial. It is suspected that the lectin pathway in *C. gigas* is likely to have undergone major changes during its evolution, and its activation cascade needs further confirmation.

In vertebrates, C3 is the central component of the complement system. It is mainly synthesized in liver and also locally macrophages, and rich in serum. C3 can be cleaved by the C3 convertases (C4bC2a) to generate C3b and C3a (40). C3b can be further cleaved by H factor and I factor into iC3b, then C3dg and C3c (41). In the present study, *Cg*C3 mRNA was expressed in all examined tissues with higher abundance in haemocytes. *Cg*C3 protein was distributed in haemolymph and haemocytes. It was cleaved to generate the fragments (*Cg*C3α, *Cg*iC3bα, and *Cg*C3γ) after *V. splendidus* stimulation.

In mammals, MBL has been identified as the main recognition molecule of the lectin pathway, which contains a conserved collagen-like domain and a CRD (36, 39). After the binding to carbohydrates *via* its CRD, MBL forms oligomer through the collagen-like region, which then activates lectin pathway (42). Glucose-binding lectin (GBL) with an N-terminus coiled-coil region instead of the collagen region is the only MBL homologue reported in tunicate *Halocynthia roretzi*, which participates in the lectin pathway (15). In the present study, *Cg*CLec-CCP identified from oyster *C. gigas* harbored an extra CCP domain, but lacked a collagen region, compared

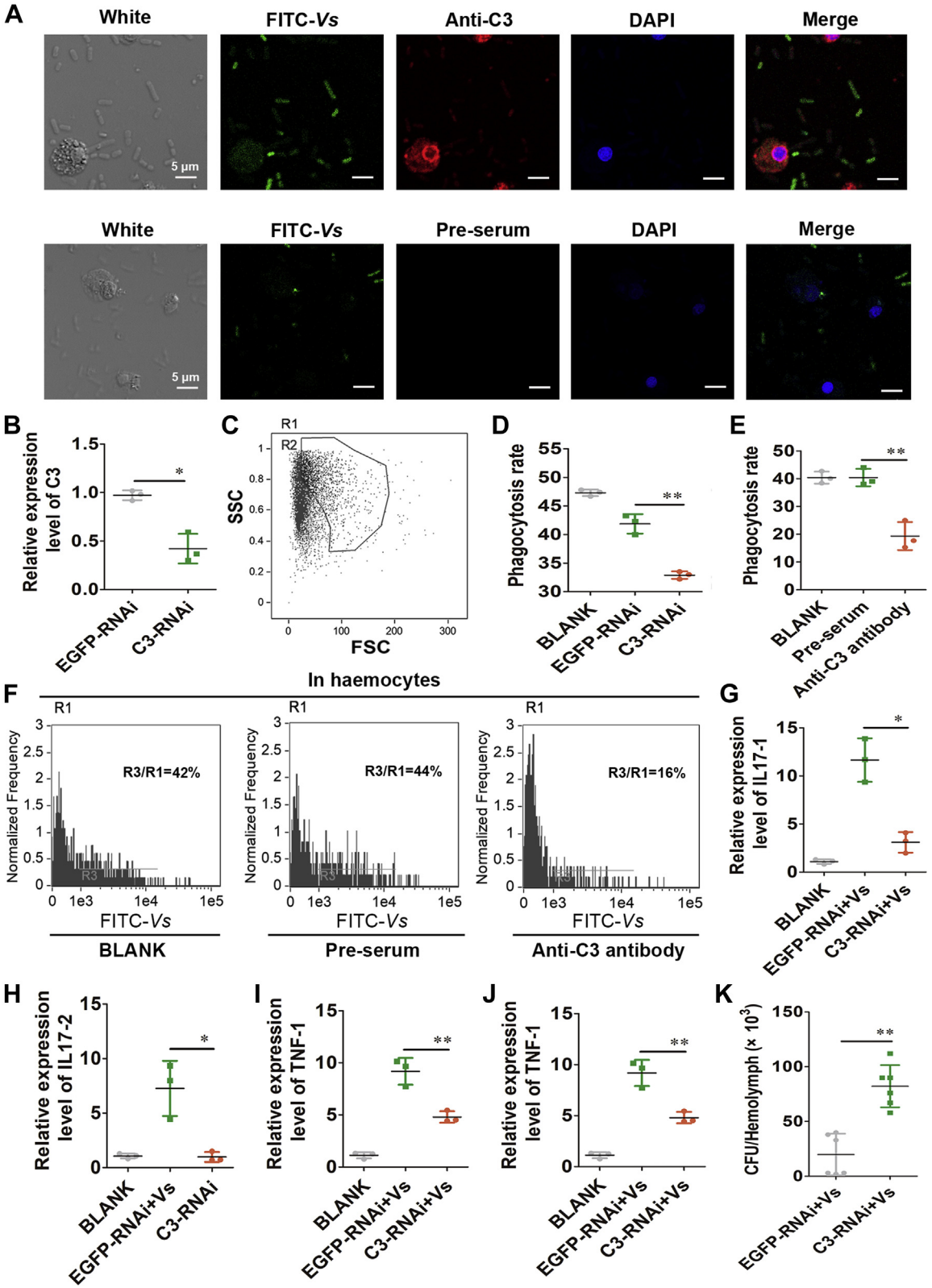

Figure 6. The haemocyte phagocytosis and immune effector expressions after *Cg*C3 was knocked or blockaded. *A*, the location of *Cg*C3 on the cell surface of *V. splendidus* by using anti-*Cg*C3 and FITC-*V. splendidus*. *B*, RNAi efficiency of *Cg*C3 in *Cg*C3 dsRNA-injection oysters using qRT-PCR. *C*, phagocytosis was detected by flow cytometry. Intact haemocytes (R2), differentiated from virions and cell debris (R1), were analyzed only in this assay. *D*, the phagocytic rate determined by flow cytometry after knockdown of *Cg*C3. *E* and *F*, the phagocytic rate determined by flow cytometry in anti-*Cg*C3-blocked oysters. Preserum was used as control. *G–J*, the mRNA transcripts of *Cg*IL17-1, *Cg*IL17-2, *Cg*TNF-1, and *Cg*BigDef1 in *Cg*C3-RNAi oysters after *V. splendidus* stimulation. *K*, the numbers of *V. splendidus* calculated in *Cg*C3-RNAi oysters. Dot plots shown were the mean ± SD (n = 3). *$p < 0.05$, **$p < 0.01$ (Student's *t* test).

with mammalian MBLs. There were six conserved residues (CPD and WPD) in the CRD of *Cg*CLec-CCP, which was suspected to bind mannose, GlcNAc, and glucose directly in the presence of Ca^{2+} similar to that of other reported MBLs (43), indicating that *Cg*CLec-CCP was a member of the mannose-binding lectin family. The *in vitro* assay confirmed that r*Cg*CLec-CCP was able to recognize different bacteria and PAMPs with a broad recognition spectrum. There is a CCP domain in *Cg*CLec-CCP, which is an evolutionarily conserved module essential for complement-mediated immune functions (44). CCP domain has been identified in several proteins of the complement system, such as B factor, C1, C2, and MASPs. In mammals, the CCP domains in MASP-2 are likely to house an exosite required for efficient cleavage of C4 by binding to the C345 C domain of C4 (45), and the CCP domain in C1r is responsible for its dimer formation (46). It is speculated that the CCP domain in *Cg*CLec-CCP may have the same function as the collagen region. As *Cg*CLec-CCP was upregulated after bacterial stimulation, our data suggest that this protein functions as a PRR to recognize bacteria and activate the complement-mediated immune response through its CCP domain.

MASP is the key component in the complement system, which mainly performs the cleavage of the complement components, such as C2, C4, and C3 (47). The homologues of mammalian MASP-1 have been identified in invertebrates, including lamprey (5) and amphioxus (13) and ascidian (16). But those identified MASP homologues from these primitive invertebrates share low similarity with mammalian MASPs. In this present study, *Cg*MASPL-1 had N-terminal CUB domains and LDLa domains, while it lacked CCP domains, compared with mammalian MASPs. The lack of the CCP in MASPL-1 might be compensated by *Cg*CLec-CCP. There were two additional cysteines (Cys683 and Cys808) in *Cg*MASPL-1 to form the "histidine loop" disulfide bridge in the protease domain, which shared the same manner as *Hs*MASP1 and *Ms*MASP1 (14). In mammals, the N-terminal CUB1-EGF-CUB2 segment of MASPs plays a key role in binding MBL or ficolins, while its C-terminal CCP1-CCP2-SP segment contributes to the catalysis of substrate cleavage (47). In the present study, r*Cg*MASPL-1-CUB1 interacted directly with *Cg*CLec-CCP *in vitro*, suggesting that the N-terminal of oyster *Cg*MASPL-1 played a similar role as mammalian MASPs in binding CTL *via* its CUB1 domain. In amphioxus, FCN1 interacts with the N-terminal CUB1-EGF-CUB2 segment of MASP1/3, indicating that there exists the classical MASPs and similar binding mechanism as that in mammals (11). The MASP family is divided into two phylogenetic lineages, TCN-type and AGY-type lineages (48). *Cg*MASPL-1 is a typical AGY-type MASP. These structural features suggested that *Cg*MASPL-1 was the orthologue of mammalian MASP-1/3 (48), and more interestingly, it lacked the conserved CCP domain, which was different from the classic complement serine proteases in other species. All these results indicated that *Cg*CLec-CCP might have evolved early as a prototype of MBL to activate *Cg*MASPL-1 in molluscs.

C3 can be cleaved by MASPs to trigger the activation of lectin pathway. Mammalian MASP1 is able to mediate the proteolytic activation of C4 and C2 to eventually induce the cleavage of C3 (47). The CCP1-CCP2-SP segment in human MASP-1 and the CCP-SP segment in amphioxus *Bj*MASP1/3 can directly activate C3 (11, 49). The MBL-MASP complex in lamprey as well as GBL-MASPa complex in ascidian is also able to activate C3 in the same manner as the human MBL-MASP1 complex (10). Even the main components of lectin pathway, such as MASP and C3, have also been found in protostomes, the existence of activable lectin pathway is still in controversy. In the present study, *Cg*CLec-CCP was found to associate *Cg*MASPL-1 in response to bacterial infection and then to cleave *Cg*C3 directly. The cleaved fragments of *Cg*C3 were similar to those of C3 in other species, suggesting that *Cg*MASPL-1 was able to directly cleave oyster *Cg*C3 (15, 39, 50). Similarly, ascidian MASPa associated with GBL was also demonstrated to cleave ascidian C3 directly (15). As there is no CCP domain in *Cg*MASPL-1, which is different from human MASP-1, amphioxus *Bj*MASP1/3, and ascidian MASPa, the cleavage mechanism of *Cg*MASPL-1 should be unique and needs further investigation. These results collectively indicated that *Cg*MASPL-1 was able to interact with C3 to promote the cleavage of C3, suggesting a new activation mechanism of C3 in molluscs and the presence of the primordial lectin pathway in primitive protostomes (18).

It is well known that C3 is cleaved by the C3 convertases to generate C3b and C3a, and C3b can bind the microbe surface to enhance cell phagocytosis (40). The phagocytic promotion mediated by C3b is currently suspected as one of the most important functions of the complement system in invertebrates (25). In ascidian and sea urchin, C3 has been reported to promote haemocyte phagocytosis toward yeast (15, 51). In the present study, the activated *Cg*C3 induced phagocytosis of oyster haemocytes, suggesting that the complement components probably functioned as opsonins to assist the haemocytes to phagocytose the opsonized pathogenic organisms (25).

It has been documented that the activation of complement lectin pathway can induce proinflammatory factor secretions and cytolysis (52). For example, C3 could mediate the IL17A secretions in mice T cells (53). In the present study, the productions of *Cg*IL17-1, *Cg*IL17-2, and *Cg*BigDef-1 in *Cg*CLec-CCP-, *Cg*MASPL-1-, or *Cg*C3-RNAi oysters were reduced after *V. splendidus* stimulation, suggesting that the ancient lectin pathway in oyster exhibited similar functions as that of mammals. For the vertebrate complement system, the most important immune reaction is to induce the cytolysis of invading pathogen. Mammalian C3b combines with C4bC2a in a covalent bond to form C5 convertases and initiate the assembly of C6 to C9 to form MACs to disturb the integrity of cell membranes of microbes (40). Because the components of C6 to C9 have not been identified in agnathans and invertebrates (7), the lytic pathway is suspected to be different from that in mammals. It has been reported that C3 in human saliva, lamprey and amphioxus humoral fluids, and haemolymph from shrimp *L. vannamei* and clam *Sinonovacula*

constricta are all essential to kill bacteria (21, 27, 54, 55). In lampreys, complement activation causes the polymerization of pore-forming protein (LPFP) and finally leads to the cytolysis of pathogens, which is distinct from the mammalian lytic pathway (7). In the present study, the activated *Cg*C3 in oyster was found to directly inhibit the bacteria growth and perforated the envelope of bacteria in haemolymph, which was different from that in mammals and lampreys (56, 57), suggesting that molluscs might have evolved an ancient cytolytic system. The results indicated that the complement system in oyster was activated by lectin pathway to induce phagocytosis, production of IL17s and defensin, and cytolysis, which played important roles in the immune defense against pathogen invasion.

In conclusion, the complete complement lectin pathway with unique activation mechanism was characterized in oyster. Upon recognizing extracellular ligands, *Cg*CLec-CCP with a CCP domain interacted with the CUB domain of *Cg*MASPL-1 to cleave *Cg*C3 directly. The activated *Cg*C3 successively mediated multiple immune responses, such as haemocyte phagocytosis, secretions of cytokines and AMPs, perforating the bacterial envelopes, and inhibition of bacterial growth and survival (Fig. 7). Defining the ancient lectin pathway, as we have done, is important to understand the activation mechanism and immune functions of complement system in invertebrates as well as the origin and evolution of mammalian complement system.

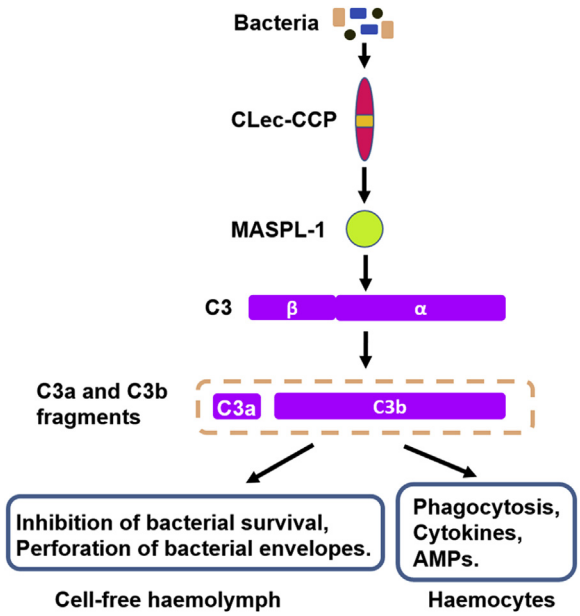

Figure 7. The scheme showing the activation cascade of ancient lectin-complement pathway in oyster. *Cg*CLec-CCP interacted with *Cg*MASPL-1 to induce the cleavage of *Cg*C3 to regulate multiple immune responses. *Cg*CLec-CCP recognized different bacteria through its CRD domain and then interacted with the CUB domain of *Cg*MASPL-1. The activated *Cg*MASPL-1 directly interacted with *Cg*C3 to induce the cleavage of *Cg*C3. The cleavage peptides of *Cg*C3 including *Cg*C3a, *Cg*C3b, *Cgi*C3b, and *Cg*C3c fragments eventually were able to inhibit the bacteria survival, perforate the bacterial envelopes in haemolymph, induce the haemocyte phagocytosis, and promote the secretions of immune effectors (cytokines and AMP).

Experimental procedures

Animals, immune stimulation, and sample collection

Pacific oysters, *C. gigas* (shell length 12–16 cm) were collected from a local breeding farm in Dalian, Liaoning, China. They were cultured in aerated seawater at 15 °C ± 2 deg. C for 14 days before processing.

The oysters individually received an injection with 100 μl of *V. splendidus* at 2×10^8 CFU/ml dissolved in PBS. Nine oysters were randomly sampled from each group at 0, 3, 6, 12, 24, 48, 72, and 96 h after *V. splendidus* stimulation. The haemolymphs collected from three oysters were pooled together as one sample, and there were three replicates for each time point. The haemocytes, as the immune cells of oysters, were collected by centrifugation at 800*g*, 4 °C for 10 min, and the total RNA was extracted using Trizol reagent (Invitrogen) to detect the temporal expression patterns of *Cg*CLec-CCP, *Cg*MASPL-1, and *Cg*C3 as the previous description (58). Tissues including muscle, gill, mantle, hepatopancreas (the important gland of certain invertebrates that combines the functions of liver and pancreas) (33), and haemolymph (the circulatory fluid of invertebrates) (34) from other nine untreated oysters were pooled as three replicates for RNA extraction to examine the mRNA distribution of the target genes in different tissues.

Gene cloning and quantitative analysis of mRNA expression

The full-length cDNA fragments of *Cg*CLec-CCP, *Cg*MASPL-1, and *Cg*C3 were obtained by PCR with the primers (Table S1) designed according to the sequence information of CGI_10008644, LOC105342011, and LOC105333243 deposited in the NCBI database (https://www.ncbi.nlm.nih.gov/), respectively. A translation tool (http://web.expasy.org/translate/) and SMART (http://smart.embl-heidelberg.de/) were used to predict the amino acid sequences and the domains in *Cg*CLec-CCP, *Cg*MASPL-1, and *Cg*C3.

qRT-PCR assays with primers of *Cg*CLec-CCP-RT, *Cg*MASPL-1-RT, and *Cg*C3-RT (Table S1) were performed to examine their expression in tissues and their temporal expression profiles in haemocytes after *V. splendidus* stimulation. The fragment of elongation factor (*Cg*EF) (NP_001292242.2) amplified with the primers of *Cg*EF-RT (Table S1) was used as an internal reference. The mRNA transcripts of interleukin 17-1 (*Cg*IL17-1), tumor necrosis factor 1 (*Cg*TNF-1), and big defensing 1 (*Cg*BigDef1) after the interference of *Cg*CLec-CCP, *Cg*MASPL-1, and *Cg*C3 were determined by using the primers of *Cg*IL17-1-RT, *Cg*IL17-1-RT, *Cg*TNF-1-RT, and *Cg*BigDef1-RT (Table S1), respectively. qRT-PCR was programmed at 95 °C for 10 min, followed by 40 cycles at 95 °C for 10 s, and 60 °C for 45 s. The final product was analyzed *via* melting analysis from 65 to 95 °C. Their relative mRNA expression levels were calculated using the $2^{-\Delta\Delta Ct}$ method (59). The data were statistically analyzed with *t* test, and the significant differences were accepted at $p < 0.05$.

Recombinant expression, purification, and antiserum production of CgCLec-CCP, CgMASPL-1, and CgC3

The recombinant proteins of *Cg*CLec-CCP (r*Cg*CLec-CCP), the N-terminal CUB domain of *Cg*MASPL-1 (r*Cg*MASPL-1-CUB1), and the NTR domain of *Cg*C3 (*Cg*C3 -NTR) were expressed in *E. coli* according to the previous report (25). The coding sequences of *Cg*CLec-CCP, *Cg*MASPL-1-CUB1, and *Cg*C3-NTR were amplified by using the primer pairs of *Cg*CLec-CCP-ExF and -ExR, *Cg*MASPL-1-CUB1-ExF and -ExR, *Cg*C3 -NTR-ExF and -ExR (Table S1), respectively. The PCR products were inserted into the pGEX-4T-1 or pET-30a expression vector and expressed in *E. coli* transetta (DE3). His-tag (rHis) from pET-32a expression vector was used as control. The recombinant proteins were purified by affinity chromatography using GST-Bind or His-Bind resin following the manufacturer's instructions. The antisera of *Cg*CLec-CCP, *Cg*MASPL-1, and *Cg*C3 were prepared as the previous report (58), which was validated by using western blotting.

The determination of CgCLec-CCP, CgMASPL-1, and CgC3 proteins by western blotting analysis

The deduced amino acid sequence of *Cg*Tubulin (NP_001292292.1) was found to be highly conserved with 81% identity to that of human beta-Tubulin (NP_001184110.1). The anti-human beta-Tubulin (AF1216, Beyotime Biotechnology) antibodies were therefore employed for western blotting assay. The proteins from cell free haemolymph and haemocytes were extracted from oysters at 30 min after *V. splendidus* stimulation, separated by 10% or 15% SDS–polyacrylamide gel electrophoresis, and then transferred onto the nitrocellulose membrane by mini transfer tank for electrophoresis. After blocked with 3% nonfat milk in TBST (10 mM Tris-HCl pH 7.5, 150 mM NaCl, 0.2% Tween-20) for 2 h, the membranes were incubated with 1/1000 diluted antisera against *Cg*CLec-CCP, *Cg*MASPL-1, and *Cg*C3 in TBST with 3% nonfat milk at room temperature for 2 h, respectively. The subsequent steps for determining *Cg*CLec-CCP, *Cg*MASPL-1, and *Cg*C3 proteins were performed as the previous report (58).

The synthesis of dsRNA and RNA interference of CgCLec-CCP, CgMASPL-1, and CgC3

The 3′-terminal cDNA sequences (about 500 bp) of *Cg*CLec-CCP, *Cg*MASPL-1, *Cg*C3, and EGFP were amplified by the primers Fi and Ri linked to the T7 promoter (Table S1) as templates to synthesize dsRNA using T7 polymerase (Takara) according to the instruction, respectively. The dsRNAs (50 μg) for *Cg*CLec-CCP, *Cg*MASPL-1, *Cg*C3, and EGFP were individually injected into each oyster. To enhance the RNAi effect, a second injection was conducted at 12 h after the first injection. Haemolymph was collected from nine oysters at 24 h after the second injection and were pooled together as three replicates (each replicate was a mixture from three individuals). At 24 h after the first injection of dsRNA, the oysters received an injection of 100 μl *V splendidus* (2×10^8 CFU/ml). The haemocytes were harvested by centrifugation, and the total RNA was extracted and assessed by qRT-PCR with specific primers RT-F and RT-R (Table S1) to evaluate the RNAi efficacy. The qRT-PCR reactions were carried out on Quan Studio 6 Flex (Thermo Fisher) using SYBR premix ExTaq (RR420, Takara, Dalian). The mRNA transcripts of *Cg*IL17-1, *Cg*IL17-1, *Cg*TNF-1, and *Cg*BigDef1 in *Cg*CLec-CCP-, *Cg*MASPL-1-, or *Cg*C3-RNAi oysters were detected at 12 h after *V. splendidus* stimulation. The relative expression levels were calculated using the $2^{-\Delta\Delta Ct}$ method (59) and statistically analyzed with *t* test. The significant differences were accepted at $p < 0.05$.

Haemolymph was obtained from three oysters at 24 h after the first injection of dsRNA and centrifuged at 400*g*, 4 °C for 10 min to collect the haemocytes, which were then incubated with *V. splendidus* for 1 h to determine the phagocytic rate of haemocytes by flow cytometry assay with Amnis ImageStream mkII and IDEAS analysis software in *Cg*CLec-CCP-, *Cg*MASPL-1-, and *Cg*C3-RNAi oysters, respectively. The phagocytic rate was the percentage of the haemocytes that phagocytosed bacteria in total haemocytes. Ten thousand haemocytes were analyzed for each sample.

At 24 h after the first injection of dsRNA, the oysters received an injection of 100 μl *V splendidus* (2×10^8 CFU/ml). The haemolymph was collected from three oysters at 1 h after *V. splendidus* stimulation and diluted 1000-fold with PBS. Each aliquot of 100 μl diluted haemolymph from *Cg*CLec-CCP-, *Cg*MASPL-1-, or *Cg*C3-RNAi oysters was cultured in a plate containing 2216E medium at 25 °C for 3 days to count the colony-forming units in the plate. The data were statistically analyzed with *t* test, and significant differences were accepted at $p < 0.05$.

The bacteria and ligand-binding assay of rCgCLec-CCP

Gram-negative bacteria (*E. coli* and *V. splendidus*) and Gram-positive bacteria (*S. aureus* and *M. luteus*) were used to test the bacterial-binding activities of rHis-*Cg*CLec-CCP with rTrx-His tag as control. Bacteria were cultured in 3 ml of Luria–Bertani (LB) medium (1% tryptone, 0.5% yeast extract, and 1% NaCl) at 37 °C overnight and then collected by centrifugation at 1000*g* for 5 min. After washed three times with TBS, the collected bacteria were resuspended in TBS and adjusted to an OD_{600} of 1.0. The bacterial suspensions (400 μl) in TBS were separately incubated with 400 μl purified rHis-*Cg*CLec-CCP (4 mM) and rTrx-His tag at room temperature with rotation for 1 h and then collected by centrifugation. The subsequent steps were carried out as the previous report (58).

An enzyme-linked immunosorbent assay (ELISA) was used to examine the activities of rHis-*Cg*CLec-CCP to directly bind pathogen-associated molecular patterns (PAMPs) (60). The wells of the microplate were coated with 50 μl (2 μg) of LPS from *E. coli*, peptidoglycan (PGN) from *S. aureus*, mannose (MAN) from yeast and glucose (GLU), and incubated at 37 °C overnight, respectively. The subsequent steps were performed as the previous report (58). Samples with P

(sample)-B (blank)/N (negative)-B (blank) > 2.1 were considered as positive. Three replications were performed for each sample, and the data were presented as mean ± SD (n = 3).

The immunocytochemical assay to determining the localization of CgC3 in haemocytes

One milliliter of oyster haemolymph was fixed with 1 ml of a mixture containing anticoagulant (pH 7.4) and 4% paraformaldehyde and then centrifuged at 600*g*, 4 °C for 10 min to collect haemocytes. The immunocytochemical assay of haemocytes was conducted as the previous description (58) with the polyclonal anti-*Cg*C3 as the primary antibody and Alexa Fluor 488-labeled Goat Anti-Mouse IgG (Beyotime Biotechnology) as the secondary antibody. The 4′-6-diamidino-2-phenylindole dihydrochloride (Beyotime Biotechnology) was used to label haemocyte nuclei. Fluorescence was observed under inversion fluorescence microscope (Axio Imager A2; ZEISS).

The confocal laser scanning microscope observation of CgC3 localization on the cell surface of V. splendidus

The haemolymph was collected from nine oysters and mixed with an anticoagulant solution (pH 7.4). The haemocytes were harvested by centrifugation at 600*g* for 10 min and resuspended in M-L15 medium at a concentration of 10^6 cell/ml. The bacteria *V. splendidus* were grown in 2216E media at 28 °C with shaking at 160 rpm for 12 h to the mid-log phase and collected *via* centrifugation at 6000*g* for 10 min. The bacteria were treated with absolute formaldehyde for 10 min, washed with NaHCO3 (0.1 M, pH 9.0) four times, and incubated with FITC (1 mg/ml; Sigma) with continuously gentle stirring at 4 °C overnight. After four times of washing with PBS, the FITC-labeled *V. splendidus* were resuspended in PBS at a concentration of 2×10^8 CFU/ml. Twenty microliters of FITC labeled *V. splendidus* was incubated with 1 ml of haemocytes in dark at room temperature with slight rotation for 0.5 h. The immunocytochemical assay of haemocytes was conducted as the previous description (58) with anti-*Cg*C3 as the primary antibody and Alexa Fluor 647-labeled Goat Anti-Mouse IgG (Beyotime Biotechnology) as the secondary antibody. Fluorescence was observed by using confocal laser scanning microscope (LSM 800, ZEISS).

Purification of native CgC3 proteins and its antibacterial activity

The proteins extracted from haemolymph and haemocytes were incubated with protein G agarose (Beyotime Biotechnology) for 10 min. The supernatants were collected by centrifugation at 400*g*, 4 °C for 10 min and then incubated with antibodies specific for *Cg*C3 at room temperature for 3 h. The mixture (bound protein and antibody) was incubated with protein G agarose at room temperature for 3 h. The resulting pellet (bound protein, antibody, and protein G agarose) was washed with TBS five times and analyzed by western blotting with the anti-*Cg*C3. Meanwhile, the pellet was also incubated with *V. splendidus* for 1 h and then the *V. splendidus* was collected for scanning electron microscope (SEM) analysis to observe the perforation of bacterial envelopes. Moreover, the antibacterial activity of the pellet was determined following the previous report (61).

The blockage assay with CgCLec-CCP and CgC3 antibodies

The blockage assay was conducted by treating the oysters with an injection of 50 μl anti-*Cg*CLec-CCP (15 mg/ml) or anti-*Cg*C3 (15 mg/ml). The oysters that received an injection with the same volume of preserum were used as the control. Another injection with 100 μl *V splendidus* (2×10^8 CFU/ml) was conducted at 1 h after the first injection with anti-*Cg*CLec-CCP. The haemolymph was collected at 2 h after *V. splendidus* stimulation, and the proteins were extracted for western blotting with anti-*Cg*C3 as mentioned above to detect the cleavage of *Cg*C3.

The anti-*Cg*C3 antibody-blocked assay was conducted to determine the phagocytic rate of haemocytes toward *V. splendidus*. Thirty minutes after the injection of anti-*Cg*C3, the oysters received another injection of 100 μl FITC-*V. splendidus* (2×10^8 CFU/ml) with the same volume of preserum as control. The haemolymph was collected from three oysters at 1 h after the injection of FITC-*V. splendidus* and centrifuged at 400*g*, 4 °C for 10 min to collect the haemocytes. The phagocytic rate of haemocytes toward FITC-*V. splendidus* was determined by flow cytometry assay.

Pull-down assay to determine the interaction between CgCLec-CCP and CgMASPL-1

The interaction between rHis-*Cg*CLec-CCP and rGST-*Cg*MASPL-1-CUB1 was determined by GST Pull-down analysis according to the previously reported method with some modification (62). Briefly, 400 μl of rGST-*Cg*MASPL-1-CUB1 (100 μg/ml) was incubated with 40 μl of Glutathione Agarose resin at room temperature for 1 h, and then 400 μl of rHis-*Cg*CLec-CCP (100 μg/ml) was added into the mixture and incubated with gentle rocking for 2 h. The mixture containing rGST-*Cg*MASPL-1-CUB1, resin, and rHis-*Cg*CLec-CCP was washed five times with TBS and then analyzed by SDS-PAGE.

Coimmunoprecipitation (Co-IP) assay

The collected oyster haemolymph was incubated with protein G for 10 min to remove nonspecific binding proteins. After centrifuged at 400*g* for 3 min, the haemolymph was incubated with anti-*Cg*CLec-CCP and anti-*Cg*MASPL-1 at room temperature for 3 h, which was then incubated with protein A + G at room temperature for 3 h, respectively. After washed with TBS for five times, the resulting pellet (bound protein, Ab, and protein G) was analyzed by western blotting using anti-*Cg*MASPL-1 and anti-*Cg*C3 antibodies as described above.

Data availability

All data generated for this study are included within this manuscript.

Supporting information—This article contains supporting information.

Acknowledgments—We are grateful to all the laboratory members for their technical advice and helpful discussions.

Author contributions—J. S., Lingling Wang, and L. S. conceptualization; J. S., Liyan Wang, and W. Y. data curation; J. S., Liyan Wang, Lingling Wang, and L. S. formal analysis; J. S., Lingling Wang, and L. S. funding acquisition; J. S., Liyan Wang, W. Y., Y. L., and Y. J. investigation; J. S., Liyan Wang, and W. Y. methodology; Lingling Wang and L. S. project administration; L. S. resources; J. S., Lingling Wang, and L. S. supervision; J. S., Lingling Wang, and L. S. validation; J. S., Liyan Wang, and W. Y. writing—original draft; J. S., Lingling Wang, and L. S. writing—review and editing.

Funding and additional information—This research was supported by National Key R&D Program (2018YFD0900502), grants (Nos. 31972817, U1706204) from National Science Foundation of China, China Agriculture Research System of MOF and MARA, the Fund for Outstanding Talents and Innovative Team of Agricultural Scientific Research from MARA, Liaoning Climbing Scholar, the Distinguished Professor of Liaoning (XLYC1902012), Key R&D Program of Liaoning Province (2017203004, 2017203001), and the Research Foundation for Talented Scholars in Dalian Ocean University (to L. W. and J. S.).

Conflict of interest—No potential conflict of interest was reported by the author(s).

Abbreviations—The abbreviations used are: A2M, alpha-2-macroglobulin family; A2MR, a-macroglobulin receptor; AMP, antimicrobial peptide; BSA, bovine serum albumin; C4bC2a, C3 convertases; CFU, colony-forming unit; Co-IP, Coimmunoprecipitation; CRD, carbohydrate recognition domain; CTL, C-type lectin; DAPI, 4′,6-diamidino-2-phenylindole; dsRNA, double-stranded RNA; FITC, fluorescein isothiocyanate; FREP, fibrinogen-related protein; GBL, glucose-binding lectin; GLU, glucose; LPS, lipopolysaccharide; MAC, membrane attack complex; MAN, mannose; MASPs, MBL-associated serine proteases; MBL, mannose-binding lectin; PAMP, pathogen-associated molecular pattern; PBS, phosphate buffered saline; PGN, peptidoglycan; PRR, pattern recognition receptor; qRT-PCR, quantitative real-time PCR; RNAi, RNA interference; SEM, scanning electron microscope; TBR, alpha-macroglobulin thiol-ester bond-forming region; TEP, thioester-containing protein; *V. splendidus*, *Vibrio splendidus*.

References

1. Hajishengallis, G., Reis, E. S., Mastellos, D. C., Ricklin, D., and Lambris, J. D. (2017) Novel mechanisms and functions of complement. *Nat. Immunol.* **18**, 1288–1298
2. Song, W. C., and FitzGerald, G. A. (2020) COVID-19, microangiopathy, hemostatic activation, and complement. *J. Clin. Invest.* **130**, 3950–3953
3. Smith, R. J. H., Appel, G. B., Blom, A. M., Cook, H. T., D'Agati, V. D., Fakhouri, F., Fremeaux-Bacchi, V., Jozsi, M., Kavanagh, D., Lambris, J. D., Noris, M., Pickering, M. C., Remuzzi, G., de Cordoba, S. R., Sethi, S., *et al.* (2019) C3 glomerulopathy - understanding a rare complement-driven renal disease. *Nat. Rev. Nephrol.* **15**, 129–143
4. Carpanini, S. M., Torvell, M., and Morgan, B. P. (2019) Therapeutic inhibition of the complement system in diseases of the central nervous system. *Front. Immunol.* **10**, 362
5. Matsushita, M., and Fujita, T. (1995) Cleavage of the third component of complement (C3) by mannose-binding protein-associated serine protease (MASP) with subsequent complement activation. *Immunobiology* **194**, 443–448
6. Spiller, F., Nycholat, C. M., Kikuchi, C., Paulson, J. C., and Macauley, M. S. (2018) Murine red blood cells lack ligands for B cell siglecs, allowing strong activation by erythrocyte surface antigens. *J. Immunol.* **200**, 949–956
7. Matsushita, M. (2018) The complement system of agnathans. *Front. Immunol.* **9**, 1405
8. Ricklin, D., Hajishengallis, G., Yang, K., and Lambris, J. D. (2010) Complement: A key system for immune surveillance and homeostasis. *Nat. Immunol.* **11**, 785–797
9. Heja, D., Kocsis, A., Dobo, J., Szilagyi, K., Szasz, R., Zavodszky, P., Pal, G., and Gal, P. (2012) Revised mechanism of complement lectin-pathway activation revealing the role of serine protease MASP-1 as the exclusive activator of MASP-2. *Proc. Natl. Acad. Sci. U. S. A.* **109**, 10498–10503
10. Takahashi, M., Iwaki, D., Matsushita, A., Nakata, M., Matsushita, M., Endo, Y., and Fujita, T. (2006) Cloning and characterization of mannose-binding lectin from lamprey (Agnathans). *J. Immunol.* **176**, 4861–4868
11. Huang, H., Huang, S., Yu, Y., Yuan, S., Li, R., Wang, X., Zhao, H., Yu, Y., Li, J., Yang, M., Xu, L., Chen, S., and Xu, A. (2011) Functional characterization of a ficolin-mediated complement pathway in amphioxus. *J. Biol. Chem.* **286**, 36739–36748
12. Nonaka, M., Fujii, T., Kaidoh, T., Natsuume-Sakai, S., Nonaka, M., Yamaguchi, N., and Takahashi, M. (1984) Purification of a lamprey complement protein homologous to the third component of the mammalian complement system. *J. Immunol.* **133**, 3242–3249
13. Endo, Y., Nonaka, M., Saiga, H., Kakinuma, Y., Matsushita, A., Takahashi, M., Matsushita, M., and Fujita, T. (2003) Origin of mannose-binding lectin-associated serine protease (MASP)-1 and MASP-3 involved in the lectin complement pathway traced back to the invertebrate, amphioxus. *J. Immunol.* **170**, 4701–4707
14. Endo, Y., Takahashi, M., Nakao, M., Saiga, H., Sekine, H., Matsushita, M., Nonaka, M., and Fujita, T. (1998) Two lineages of mannose-binding lectin-associated serine protease (MASP) in vertebrates. *J. Immunol.* **161**, 4924–4930
15. Sekine, H., Kenjo, A., Azumi, K., Ohi, G., Takahashi, M., Kasukawa, R., Ichikawa, N., Nakata, M., Mizuochi, T., Matsushita, M., Endo, Y., and Fujita, T. (2001) An ancient lectin-dependent complement system in an ascidian: Novel lectin isolated from the plasma of the solitary ascidian, Halocynthia roretzi. *J. Immunol.* **167**, 4504–4510
16. Ji, X., Azumi, K., Sasaki, M., and Nonaka, M. (1997) Ancient origin of the complement lectin pathway revealed by molecular cloning of mannan binding protein-associated serine protease from a urochordate, the Japanese ascidian, Halocynthia roretzi. *Proc. Natl. Acad. Sci. U. S. A.* **94**, 6340–6345
17. Nonaka, M., Azumi, K., Ji, X., Namikawa-Yamada, C., Sasaki, M., Saiga, H., Dodds, A. W., Sekine, H., Homma, M. K., Matsushita, M., Endo, Y., and Fujita, T. (1999) Opsonic complement component C3 in the solitary ascidian, *Halocynthia roretzi*. *J. Immunol.* **162**, 387–391
18. Skjoedt, M. O., Palarasah, Y., Rasmussen, K., Vitved, L., Salomonsen, J., Kliem, A., Hansen, S., Koch, C., and Skjodt, K. (2010) Two mannose-binding lectin homologues and an MBL-associated serine protease are expressed in the gut epithelia of the urochordate species *Ciona intestinalis*. *Dev. Comp. Immunol.* **34**, 59–68
19. Dodds, A. W. (2002) Which came first, the lectin/classical pathway or the alternative pathway of complement? *Immunobiology* **205**, 340–354
20. Golrokh Mofrad, M., Taghizadeh Maleki, D., and Faghihloo, E. (2020) The roles of programmed death ligand 1 in virus-associated cancers. *Infect. Genet. Evol.* **84**, 104368
21. Liu, Y., Song, Q., Li, D., Zou, R., Zhang, Y., Hao, S., Geng, X., and Sun, J. (2019) A novel complement C3 like gene (Lv-C3L) from *Litopenaeus*

vannamei with bacteriolytic and hemolytic activities and its role in antiviral immune response. *Fish Shellfish Immunol.* **91**, 376–387
22. Nonaka, M., and Kimura, A. (2006) Genomic view of the evolution of the complement system. *Immunogenetics* **58**, 701–713
23. Kimura, A., Sakaguchi, E., and Nonaka, M. (2009) Multi-component complement system of Cnidaria: C3, Bf, and MASP genes expressed in the endodermal tissues of a sea anemone, Nematostella vectensis. *Immunobiology* **214**, 165–178
24. Satoh, H., Oshiro, N., Iwanaga, S., Namikoshi, M., and Nagai, H. (2007) Characterization of PsTX-60B, a new membrane-attack complex/perforin (MACPF) family toxin, from the venomous sea anemone *Phyllodiscus semoni*. *Toxicon* **49**, 1208–1210
25. Wang, L., Zhang, H., Wang, L., Zhang, D., Lv, Z., Liu, Z., Wang, W., Zhou, Z., Qiu, L., Wang, H., Li, J., and Song, L. (2017) The RNA-seq analysis suggests a potential multi-component complement system in oyster *Crassostrea gigas*. *Dev. Comp. Immunol.* **76**, 209–219
26. Prado-Alvarez, M., Rotllant, J., Gestal, C., Novoa, B., and Figueras, A. (2009) Characterization of a C3 and a factor B-like in the carpet-shell clam, *Ruditapes decussatus*. *Fish Shellfish Immunol.* **26**, 305–315
27. Peng, M., Niu, D., Wang, F., Chen, Z., and Li, J. (2016) Complement C3 gene: Expression characterization and innate immune response in razor clam *Sinonovacula constricta*. *Fish Shellfish Immunol.* **55**, 223–232
28. Peng, M., Niu, D., Chen, Z., Lan, T., Dong, Z., Tran, T. N., and Li, J. (2017) Expression of a novel complement C3 gene in the razor clam *Sinonovacula constricta* and its role in innate immune response and hemolysis. *Dev. Comp. Immunol.* **73**, 184–192
29. Gerdol, M., and Venier, P. (2015) An updated molecular basis for mussel immunity. *Fish Shellfish Immunol.* **46**, 17–38
30. Li, H., Zhang, H., Jiang, S., Wang, W., Xin, L., Wang, H., Wang, L., and Song, L. (2015) A single-CRD C-type lectin from oyster *Crassostrea gigas* mediates immune recognition and pathogen elimination with a potential role in the activation of complement system. *Fish Shellfish Immunol.* **44**, 566–575
31. Gorbushin, A. M. (2019) Derivatives of the lectin complement pathway in Lophotrochozoa. *Dev. Comp. Immunol.* **94**, 35–58
32. Cerenius, L., Kawabata, S., Lee, B. L., Nonaka, M., and Soderhall, K. (2010) Proteolytic cascades and their involvement in invertebrate immunity. *Trends Biochem. Sci.* **35**, 575–583
33. Zhang, G., Fang, X., Guo, X., Li, L., Luo, R., Xu, F., Yang, P., Zhang, L., Wang, X., Qi, H., Xiong, Z., Que, H., Xie, Y., Holland, P. W., Paps, J., *et al.* (2012) The oyster genome reveals stress adaptation and complexity of shell formation. *Nature* **490**, 49–54
34. Walport, M. J. (2001) Complement. First of two parts. *N. Engl. J. Med.* **344**, 1058–1066
35. Kinoshita, T. (1991) Biology of complement: The overture. *Immunol. Today* **12**, 291–295
36. Fujita, T., Matsushita, M., and Endo, Y. (2004) The lectin-complement pathway–its role in innate immunity and evolution. *Immunol. Rev.* **198**, 185–202
37. Azumi, K., De Santis, R., De Tomaso, A., Rigoutsos, I., Yoshizaki, F., Pinto, M. R., Marino, R., Shida, K., Ikeda, M., Arai, M., Inoue, Y., Shimizu, T., Satoh, N., Rokhsar, D. S., Du Pasquier, L., *et al.* (2003) Genomic analysis of immunity in a urochordate and the emergence of the vertebrate immune system: "Waiting for Godot". *Immunogenetics* **55**, 570–581
38. Huang, S., Yuan, S., Guo, L., Yu, Y., Li, J., Wu, T., Liu, T., Yang, M., Wu, K., and Liu, H. (2008) Genomic analysis of the immune gene repertoire of amphioxus reveals extraordinary innate complexity and diversity. *Genome Res.* **18**, 1112
39. Matsushita, M., Matsushita, A., Endo, Y., Nakata, M., Kojima, N., Mizuochi, T., and Fujita, T. (2004) Origin of the classical complement pathway: Lamprey orthologue of mammalian C1q acts as a lectin. *Proc. Natl. Acad. Sci. U. S. A.* **101**, 10127–10131
40. Nonaka, M., and Yoshizaki, F. (2004) Evolution of the complement system. *Mol. Immunol.* **40**, 897–902
41. Kim, H. M., and Kim, Y. M. (2018) HMGB1: LPS delivery vehicle for caspase-11-mediated pyroptosis. *Immunity* **49**, 582–584
42. Pinto, M. R., Melillo, D., Giacomelli, S., Sfyroera, G., and Lambris, J. D. (2007) Ancient origin of the complement system: Emerging invertebrate models. *Adv. Exp. Med. Biol.* **598**, 372–388
43. Fong, J. J., Tsai, C. M., Saha, S., Nizet, V., Varki, A., and Bui, J. D. (2018) Siglec-7 engagement by GBS beta-protein suppresses pyroptotic cell death of natural killer cells. *Proc. Natl. Acad. Sci. U. S. A.* **115**, 10410–10415
44. Dempsey, P. W., Allison, M. E., Akkaraju, S., Goodnow, C. C., and Fearon, D. T. (1996) C3d of complement as a molecular adjuvant: Bridging innate and acquired immunity. *Science* **271**, 348–350
45. Kidmose, R. T., Laursen, N. S., Dobo, J., Kjaer, T. R., Sirotkina, S., Yatime, L., Sottrup-Jensen, L., Thiel, S., Gal, P., and Andersen, G. R. (2012) Structural basis for activation of the complement system by component C4 cleavage. *Proc. Natl. Acad. Sci. U. S. A.* **109**, 15425–15430
46. Gao, J., Wei, B., de Assuncao, T. M., Liu, Z., Hu, X., Ibrahim, S., Cooper, S. A., Cao, S., Shah, V. H., and Kostallari, E. (2020) Hepatic stellate cell autophagy inhibits extracellular vesicle release to attenuate liver fibrosis. *J. Hepatol.* **73**, 1144–1154
47. Yongqing, T., Drentin, N., Duncan, R. C., Wijeyewickrema, L. C., and Pike, R. N. (2012) Mannose-binding lectin serine proteases and associated proteins of the lectin pathway of complement: Two genes, five proteins and many functions? *Biochim. Biophys. Acta* **1824**, 253–262
48. Fujita, T. (2002) Evolution of the lectin-complement pathway and its role in innate immunity. *Nat. Rev. Immunol.* **2**, 346–353
49. Matsushita, M., Thiel, S., Jensenius, J. C., Terai, I., and Fujita, T. (2000) Proteolytic activities of two types of mannose-binding lectin-associated serine protease. *J. Immunol.* **165**, 2637–2642
50. Tzeng, S. J., Bolland, S., Inabe, K., Kurosaki, T., and Pierce, S. K. (2005) The B cell inhibitory Fc receptor triggers apoptosis by a novel c-Abl family kinase-dependent pathway. *J. Biol. Chem.* **280**, 35247–35254
51. Ricklin, D., Reis, E. S., and Lambris, J. D. (2016) Complement in disease: A defence system turning offensive. *Nat. Rev. Nephrol.* **12**, 383–401
52. Sarma, J. V., and Ward, P. A. (2011) The complement system. *Cell Tissue Res.* **343**, 227–235
53. Byrne, A. B., and Talarico, L. B. (2021) Role of the complement system in antibody-dependent enhancement of flavivirus infections. *Int. J. Infect. Dis.* **103**, 404–411
54. von Gunten, S., Yousefi, S., Seitz, M., Jakob, S. M., Schaffner, T., Seger, R., Takala, J., Villiger, P. M., and Simon, H. U. (2005) Siglec-9 transduces apoptotic and nonapoptotic death signals into neutrophils depending on the proinflammatory cytokine environment. *Blood* **106**, 1423–1431
55. Lu, C., Guo, C., Chen, H., Zhang, H., Zhi, L., Lv, T., Li, M., Niu, Z., Lu, P., and Zhu, W. (2020) A novel chimeric PD1-NKG2D-41BB receptor enhances antitumor activity of NK92 cells against human lung cancer H1299 cells by triggering pyroptosis. *Mol. Immunol.* **122**, 200–206
56. Gros, P., Milder, F. J., and Janssen, B. J. (2008) Complement driven by conformational changes. *Nat. Rev. Immunol.* **8**, 48–58
57. Pangburn, M. K., and Rawal, N. (2002) Structure and function of complement C5 convertase enzymes. *Biochem. Soc. Trans.* **30**, 1006–1010
58. Marasco, M., Berteotti, A., Weyershaeuser, J., Thorausch, N., Sikorska, J., Krausze, J., Brandt, H. J., Kirkpatrick, J., Rios, P., Schamel, W. W., Kohn, M., and Carlomagno, T. (2020) Molecular mechanism of SHP2 activation by PD-1 stimulation. *Sci. Adv.* **6**, eaay4458
59. Livak, K. J., and Schmittgen, T. D. (2001) Analysis of relative gene expression data using real-time quantitative PCR and the 2(-Delta Delta C(T)) method. *Methods* **25**, 402–408
60. Sun, J., Wang, L., Huang, M., Li, Y., Wang, W., and Song, L. (2019) CgCLec-HTM-mediated signaling pathway regulates lipopolysaccharide-induced CgIL-17 and CgTNF production in oyster. *J. Immunol.* **203**, 1845–1856
61. Sun, J. J., Lan, J. F., Zhao, X. F., Vasta, G. R., and Wang, J. X. (2017) Binding of a C-type lectin's coiled-coil domain to the Domeless receptor directly activates the JAK/STAT pathway in the shrimp immune response to bacterial infection. *PLoS Pathog.* **13**, e1006626
62. Sun, J. J., Lan, J. F., Shi, X. Z., Yang, M. C., Niu, G. J., Ding, D., Zhao, X. F., Yu, X. Q., and Wang, J. X. (2016) Beta-arrestins negatively regulate the toll pathway in shrimp by preventing dorsal translocation and inhibiting dorsal transcriptional activity. *J. Biol. Chem.* **291**, 7488–7504